Advances in Applied Mathematics and Mechanics
Adv. Appl. Math. Mech., Vol. **2**, No. 6, pp. 784-797

DOI: 10.4208/aamm.09-m09110
December 2010

A Modified Nonconforming 5-Node Quadrilateral Transition Finite Element

Feiteng Huang[1] and Xiaoping Xie[1,*]

[1] *School of Mathematics, Sichuan University, Chengdu 610064, China*

Received 18 December 2009; Accepted (in revised version) 9 May 2010
Available online 26 August 2010

Abstract. This paper analyzes a nonconforming 5-node quadrilateral transition finite element for Poisson equation. This element was originally proposed by Choi and Park [Computers and Structures, 32 (1989), pp. 295–304 and Thin-Walled Structures, 28 (1997), pp. 1–20] for the analysis of Mindlin plates. We show the consistency error of this element is only $\mathcal{O}(h^{1/2})$ over the transition edges of the quadrilateral subdivision. By modifying the shape functions with respect to mid-nodes, we get an improved version of the element for which the consistency error is $\mathcal{O}(h)$. Numerical examples are provided to verify the theoretical results.

AMS subject classifications: 65N12, 65N30

Key words: Nonconforming finite element, transition element, consistency error.

1 Introduction

Adaptive methods for the numerical solution of the PDEs are now standard tools in science and engineering to achieve better accuracy with minimum degrees of freedom. In the adaptive analysis, the mesh is locally refined according to the estimated error distribution through repeating the working loop comprised of finite element analysis, error estimation, element or edge marking and mesh refinement until the error decreases to a prescribed level.

As far as adaptive quadrilateral mesh refinement is concerned, when a 4-node quadrilateral element is subdivided into smaller elements, new nodes (hanging nodes) appear on the boundaries of its immediate neighborhoods, which are known as transition elements. In these elements, each edge may possess a mid-side node and the edge is shared by the adjacent bilinear elements. When the conventional quadratic interpolation is used along the 3-node edge, interelement compatibility is violated. There are several ways to secure this [8, 16].

*Corresponding author.
Email: hftenger@126.com (F. T. Huang), xpxiec@gmail.com (X. P. Xie)

The first way is to constrain the mid-side node displacement of the transition element to be the average of the displacement at the two corner nodes of the same edge (Fig. 1(a): $u_c=(u_a+u_b)/2$) [19, 20]. However, this nullifies the accuracy enhancement effect of the mid-side nodes and constraint equations are computationally inefficient [1].

The second way is to use a meshing technique of finite element layout shown in Fig. 1(b). In this case, no constraints are imposed, but the use of distorted elements is inevitable.

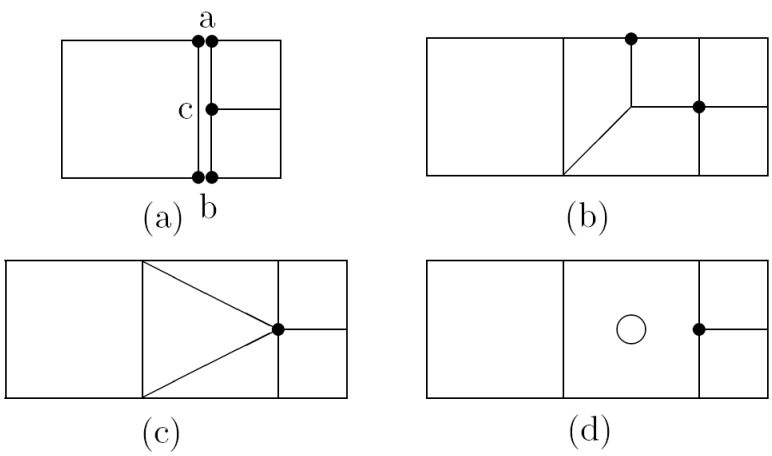

Figure 1: Examples of mesh transition.

The third way is to use macro-elements formed by compatible 4-node bilinear quadrilaterals and compatible 3-node linear triangles (Fig. 1(c)). Since the triangular elements produce worse results than the quadrilaterals in general, the introduction of triangular elements in the mesh may cause poor solutions even if the quadrilaterals in the mesh behave well.

The fourth way is to introduce transition elements (Fig. 1(d)) to connect directly the different layer patterns. Well-established transition element can overcome some of the aforementioned meshing problems. Gupta [13] derived a set of compatible interpolation functions for the quadrilateral transition elements. The displacement interpolation along a 3-node element edge is continuous piecewise bilinear instead of quadratic, thus preserve the interelement compatibility. Carstensen and Hu [5] provided a method to preseve the interelement compatibility with just modifying the nodal basis functions of the immediate neighborhoods of the hanging nodes. McDill [17] and Morton [18] presented the 3D counterpart of Gupta's conforming transition elements. Choi et al. [6–9] proposed a set of 2D and 3D nonconforming transition elements. Wan et al. [16, 21], Wu et al. [22], Duan et al. [11], Hasan et al. [14] and Peters et al. [19] constructed some hybrid stress and enhanced strain transition quadrilateral/hexahedral elements.

In this paper, we shall analyze the nonconforming 5-node quadrilateral transition

finite element proposed by Choi and Park [8] and then derive its improved version. To simplify the analysis, we consider the Poisson problem

$$\begin{cases} -\Delta u = f, & \text{in } \Omega, \\ u|_{\Gamma_D} = 0, & \nabla u \cdot \mathbf{n}|_{\Gamma_N} = g, \end{cases} \tag{1.1}$$

where $\Omega \in \Re^2$ is a polygonal domain with boundary

$$\begin{aligned} &\partial\Omega = \Gamma_D \bigcup \Gamma_N, \qquad && \text{meas}(\Gamma_D) > 0, \\ &f \in L^2(\Omega), && g \in H^{-1/2}(\Gamma_N). \end{aligned}$$

The weak formulation for this problem reads as: find

$$u \in V := \Big\{ v \in H^1(\Omega) : \ v|_{\Gamma_D} = 0 \Big\},$$

such that

$$\int_\Omega \nabla u \cdot \nabla v \mathrm{d}x = F(v), \quad \forall v \in V, \tag{1.2}$$

where

$$F(v) := \int_\Omega f \cdot v \mathrm{d}x + \int_{\Gamma_N} g \cdot v \mathrm{d}s.$$

The rest of this paper is organized as follows. In Section 2, we derive an error estimate for the nonconforming 5-node quadrilateral transition element and in Section 3 we give an improved version of the element. We finally do numerical tests to verify our analysis in Section 4.

2 Error analysis for nonconforming 5-node quadrilateral transition element

2.1 Finite element construction

Let $\mathcal{T}_h$ be a shape regular subdivision of Ω into quadrilaterals. Let $K \in \mathcal{T}_h$ be an arbitrary quadrilateral with diameter h_K. Denote

$$h := \max_{K \in \mathcal{T}_h} \{h_K\},$$

we define the isoparametric bilinear mapping $F_K : \widehat{K} = [-1,1]^2 \longrightarrow K$ (see Fig. 2) as

$$\begin{pmatrix} x \\ y \end{pmatrix} = F_K(\xi, \eta) = \frac{1}{4} \sum_{i=1}^{4} (1 + \xi_i \xi)(1 + \eta_i \eta),$$

where ξ, η are the local isoparametric coordinates and

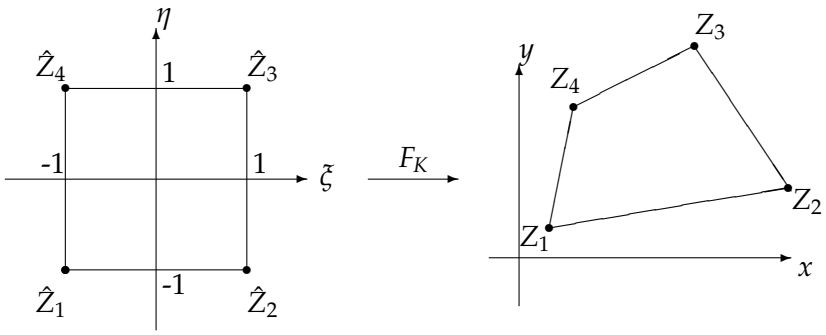

Figure 2: The mapping F_K.

$$\begin{pmatrix} \xi_1 & \xi_2 & \xi_3 & \xi_4 \\ \eta_1 & \eta_2 & \eta_3 & \eta_4 \end{pmatrix} = \begin{pmatrix} -1 & 1 & 1 & -1 \\ -1 & -1 & 1 & 1 \end{pmatrix}.$$

Let v_i $(i = 1, \cdots, 5)$ be the nodal values at the four vertices, Z_i $(i = 1, \cdots, 4)$ of K and one mid-side node Z_5. The corresponding referential mid-side nodal $\hat{Z}_5$ falls into four cases as shown in Fig. 3. The interpolation function v_{tr} on the transition element K has the form [8]

$$\widehat{v}_{tr} = v_{tr} \circ F_K = \sum_{i=1}^{5} N_i v_i. \tag{2.1}$$

Here the mid-side nodal basis N_5 is taken as

$$N_5 = \widetilde{N}_i, \quad \text{if the } i\text{-th mid-side point is a node (Fig. 3),}$$

where $i = 5, \cdots, 8$ and

$$\widetilde{N}_5 = \frac{1}{2}(1+\xi)(1-\eta^2), \quad \widetilde{N}_6 = \frac{1}{2}(1+\eta)(1-\xi^2), \tag{2.2a}$$

$$\widetilde{N}_7 = \frac{1}{2}(1-\xi)(1-\eta^2), \quad \widetilde{N}_8 = \frac{1}{2}(1-\eta)(1-\xi^2). \tag{2.2b}$$

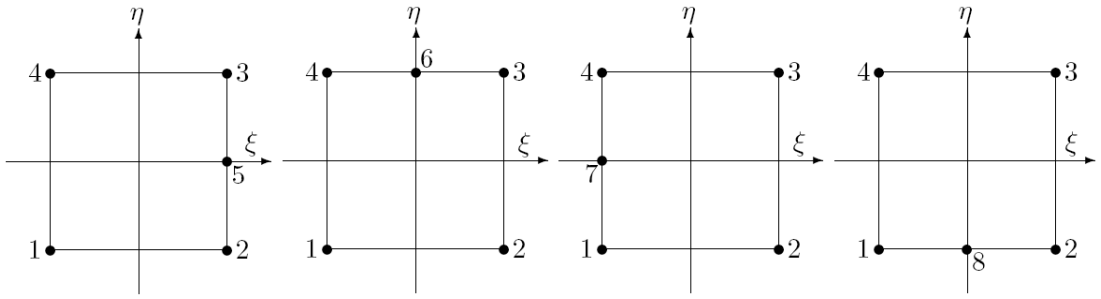

Figure 3: Node number system for transition elements.

Especially, we take $\widetilde{N}_i = 0$, if the i-th mid-side point is not a node for $i = 5, \cdots, 8$. The vertex nodal basis N_i are then given by

$$N_1 = \frac{1}{4}(1-\xi)(1-\eta) - \frac{1}{2}(\widetilde{N}_7 + \widetilde{N}_8), \quad N_2 = \frac{1}{4}(1+\xi)(1-\eta) - \frac{1}{2}(\widetilde{N}_8 + \widetilde{N}_5), \tag{2.3a}$$

$$N_3 = \frac{1}{4}(1+\xi)(1+\eta) - \frac{1}{2}(\widetilde{N}_5 + \widetilde{N}_6), \quad N_4 = \frac{1}{4}(1-\xi)(1+\eta) - \frac{1}{2}(\widetilde{N}_6 + \widetilde{N}_7). \tag{2.3b}$$

Remark 2.1. From the basis functions (2.2)-(2.3), we easily know that for any edge $\hat{e}$ of $\hat{K}$

$$\widehat{v}_{tr}|_{\hat{e}} \text{ is } \begin{cases} \text{a linear function in } \xi, \eta, & \text{if } \hat{e} \text{ has only 2 nodes,} \\ \text{a quadratic function in } \xi, \eta, & \text{if } \hat{e} \text{ has 3 nodes.} \end{cases}$$

Remark 2.2. For Gupta's conforming transition element [13],

$$\widetilde{N}_5 = \frac{1}{2}(1+\xi)(1-|\eta|), \quad \widetilde{N}_6 = \frac{1}{2}(1+\eta)(1-|\xi|),$$
$$\widetilde{N}_7 = \frac{1}{2}(1-\xi)(1-|\eta|), \quad \widetilde{N}_8 = \frac{1}{2}(1-\eta)(1-|\xi|).$$

Remark 2.3. When K is a 4-node quadrilateral element, the isoparametric bilinear interpolation v_{bi} is given by

$$\widehat{v}_{bi} = v_{bi} \circ F_K = \frac{1}{4}\sum_{i=1}^{4}(1+\xi_i\xi)(1+\eta_i\eta)v_i. \tag{2.4}$$

Let V_h be finite dimensional space defined as

$$V_h := \Big\{ v : v|_{\Gamma_D} = 0, v \text{ is continuous at all the vertices of the quadrilateral mesh } \mathcal{T}_h,$$
$$v|_K = \begin{cases} v_{tr}, & \text{if } K \text{ is a 5-node transition element for all } K \in \mathcal{T}_h, \\ v_{bi}, & \text{if } K \text{ is a 4-node quadrilateral element for all } K \in \mathcal{T}_h, \end{cases} \Big\}, \tag{2.5}$$

where v_{tr}, v_{bi} are given by (2.1), (2.4) respectively. It is easy to know V_h contains continuous piecewise isoparametric bilinear interpolation functions, namely

$$V_h \supset V_h^c := \Big\{ v \in C^0(\overline{\Omega}) : \widehat{v} = v|_K \circ F_K \in \text{ span}\{1, \xi, \eta, \xi\eta\}, \text{ for all } K \in \mathcal{T}_h \Big\}. \tag{2.6}$$

Then the corresponding finite element scheme for the problem (1.2) reads as: find $u_h \in V_h$, such that

$$\int_\Omega \nabla_h u_h \cdot \nabla_h v \mathrm{d}x = F(v), \quad \text{for all } v \in V_h. \tag{2.7}$$

2.2 Error analysis

Define

$$(v,w)_h := \sum_{K\in\mathcal{T}_h}\int_K \nabla v\cdot\nabla w\mathrm{d}x, \quad \text{for } v,w\in V_h+V,$$
$$\|v\|_h := \big((v,v)_h\big)^{\frac{1}{2}}.$$

In the following, we use, for convenience, the notation $a \lesssim b$ to represent that there exists a generic positive constant C, independent of the mesh parameter h, such that $a \le Cb$.

According to the theory of nonconforming finite element methods (cf. [2, 10]), it holds the following result.

Lemma 2.1. *Let $u \in V$ be the solution of the variational problem* (1.2)*. Then the discretization problem* (2.7) *admits a unique solution $u_h \in V_h$, such that*

$$\|u-u_h\|_h \le \inf_{v\in V_h}\|u-v\|_h + \sup_{w\in V_h\setminus\{0\}}\frac{\big|(u-u_h,w)_h\big|}{\|w\|_h}. \tag{2.8}$$

For the approximation error term $\inf_{v\in V_h}\|u-v\|_h$, from the relation (2.6) it holds

$$\inf_{v\in V_h}\|u-v\|_h \le \inf_{v\in V_h^c}|u-v|_{1,\Omega}. \tag{2.9}$$

Here and in what follows, we use $\|\cdot\|_{k,T}$ and $|\cdot|_{k,T}$ to denote the usual norm and seminorm on the Sobolev space $H^k(T)$.

By (2.9), we only need to analyze the consistency error term

$$\sup_{w\in V_h\setminus\{0\}}\frac{\big|(u-u_h,w)_h\big|}{\|w\|_h},$$

from integration by parts and Remark 2.1, we have

$$\begin{aligned}(u-u_h,w)_h &= \sum_{K\in\mathcal{T}_h}\int_K \nabla u\cdot\nabla w\mathrm{d}x - \int_\Omega f\,w\mathrm{d}x\\ &= \sum_{K\in\mathcal{T}_h}\Big(\int_{\partial K}\nabla u\cdot\mathbf{n}\,w\mathrm{d}s - \int_K \Delta u\,w\mathrm{d}x\Big) - \int_\Omega f\,w\mathrm{d}x\\ &= \sum_{K\in\mathcal{T}_h}\int_{\partial K}\nabla u\cdot\mathbf{n}\,w\mathrm{d}s = \sum_{e\in\mathcal{E}_h^*}\int_e \nabla u\cdot\mathbf{n}[w]\mathrm{d}s,\end{aligned} \tag{2.10}$$

where $\mathcal{E}_h^*$ is the set of 3-node edges of all transition elements in $\mathcal{T}_h$, $\mathbf{n}$ is the unit outer normal and $[w]$ is the jump of w across e. Then we only need to estimate (2.10).

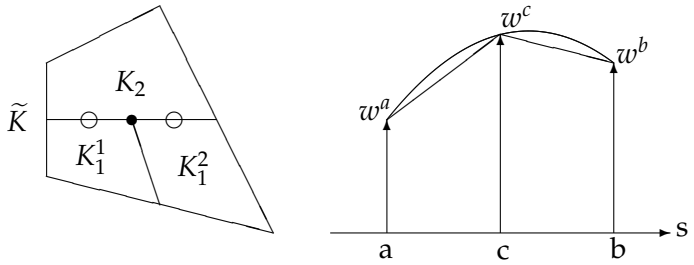

Figure 4: Interpolation function along the 3-node edge of a transition element.

Consider a transition element K_2 with two adjacent 4-node element K_1^1, K_1^2 (see Fig. 4). Denote

$$K_1 := K_1^1 \bigcup K_1^2, \qquad \widetilde{K} := K_1 \bigcup K_2,$$
$$e_i := \overline{K_1^i} \bigcap \overline{K_2}, \qquad e := e_1 \bigcup e_2,$$

where $i = 1, 2$. Let a, b, c be the three nodes of the edge e. Since $[w]$ vanishes at the nodes a, b, c and $\big(w|_{K_1^i}\big)\big|_{e_i}$ is a linear function for $i = 1, 2$, from a standard scaling argument together with trace inequality, we have

$$\big|[w]\big|_{0,e}^2 \lesssim h|w|_{1,\widetilde{K}}^2. \tag{2.11}$$

Therefore, it follows

$$\Big|\sum_{e\in\mathcal{E}_h^*}\int_e \nabla u\cdot\mathbf{n}[w]\mathrm{d}s\Big| \le \Big(\sum_{e\in\mathcal{E}_h^*}|u|_{1,e}^2\Big)^{\frac{1}{2}}\Big(\sum_{e\in\mathcal{E}_h^*}\big|[w]\big|_{0,e}^2\Big)^{\frac{1}{2}} \lesssim h^{\frac{1}{2}}|u|_{1,\mathcal{E}_h^*}\|w\|_h,$$

where

$$|u|_{1,\mathcal{E}_h^*} := \Big(\sum_{e\in\mathcal{E}_h^*}|u|_{1,e}^2\Big)^{\frac{1}{2}}.$$

This indicates

$$\sup_{w\in V_h\setminus\{0\}}\frac{\big|(u-u_h,w)_h\big|}{\|w\|_h} \lesssim h^{\frac{1}{2}}|u|_{1,\mathcal{E}_h^*}. \tag{2.12}$$

From Lemma 2.1, Eqs. (2.9), (2.12) and the standard interpolation theory, we obtain the following conclusion.

Proposition 2.1. *Let $u \in V\bigcap H^2(\Omega)$ and $u_h \in V_h$ be respectively the solutions of the weak problem* (1.2) *and of the discretized problem* (2.7)*. Then it holds*

$$\|u-u_h\|_h \lesssim h|u|_{2,\Omega} + h^{\frac{1}{2}}|u|_{1,\mathcal{E}_h^*}.$$

From this proposition we know that the error estimate for the nonconforming 5-node transition element is, in some sense, not optimal due to the $h^{1/2}$-loss of accuracy for the consistency error term. In next section we shall discuss improvement of this transition element.

3 Modified nonconforming transition element

From the finite element construction in the above section, we know the interpolation function on the original nonconforming transition element and its two adjacent 4-node elements is continuous at the mid-side node as well as at the two endpoint nodes of the transition edge (see Fig. 4). This, however, leads to $h^{1/2}$-loss of accuracy, as shown in Proposition 2.1. In this section, we shall modify the element by replacing the continuity of interpolation at mide-side nodes with the continuity of mean value over any transition edge e, namely

$$\int_e [w]\mathrm{d}s = 0, \quad \text{for all } w \in V_h. \tag{3.1}$$

Remark 3.1. For the original nonconforming transition element, a combination of (2.11) and Hölder inequality yields

$$\Big| \int_e [w]\mathrm{d}s \Big| \le h^{\frac{1}{2}} \big| [w] \big|_{0,e} \lesssim h|w|_{1,\widetilde{K}}. \tag{3.2}$$

To arrive at (3.1) it suffices to modify the nodal basis functions in (2.2) as follows:

$$\widetilde{N_5} = \frac{3}{8}(1+\xi)(1-\eta^2), \quad \widetilde{N_6} = \frac{3}{8}(1+\eta)(1-\xi^2), \tag{3.3a}$$

$$\widetilde{N_7} = \frac{3}{8}(1-\xi)(1-\eta^2), \quad \widetilde{N_8} = \frac{3}{8}(1-\eta)(1-\xi^2). \tag{3.3b}$$

Remark 3.2. Notice that in this case $N_5 = \widetilde{N_i}$ is not the nodal basis corresponding to the mid-side node i for $i = 5, \cdots, 8$.

Lemma 3.1. *For the modified nonconforming element, it holds the relation* (3.1) *and*

$$\sup_{w \in V_h \setminus \{0\}} \frac{\big|(u-u_h, w)_h\big|}{\|w\|_h} \lesssim h|u|_{2,\mathcal{T}_h^*}, \tag{3.4}$$

where $\mathcal{T}_h^*$ is the set of all macro-elements like $\widetilde{K}$ in Fig. 5, each of which consists of a transition element and its two adjacent 4-node quadrilateral elements sharing the transition edge,

$$|u|_{2,\mathcal{T}_h^*} := \Big(\sum_{\widetilde{K} \in \mathcal{T}_h^*} |u|^2_{2,\widetilde{K}} \Big)^{\frac{1}{2}}.$$

Proof. For $w \in V_h$, let w^a, w^b be the nodal values of w at the two endpoint nodes a, b and let w_1^c, w_2^c be respectively the nodal values of $w|_{K_1}$ and $w|_{K_2}$ at the mid-side node c (Fig. 5). From (3.3), (2.3) and (2.1), we easily have

$$w_2^c = \frac{3}{4} w_1^c + \frac{1}{8}(w^a + w^b). \tag{3.5}$$

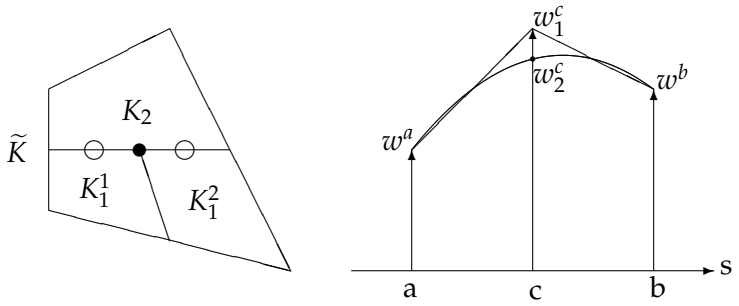

Figure 5: Interpolation function along the 3-node edge of a modified transition element.

Denote

$$f_1 := \big(w|_{K_1}\big)\big|_e, \quad f_2 := \big(w|_{K_2}\big)\big|_e, \quad h_{ab} = \text{length}(e),$$

then by (2.4) and (2.1), we have

$$\begin{aligned}
\int_e f_1 \mathrm{d}s =& \frac{1}{4}w^a h_{ab} + \frac{1}{4}w_1^c h_{ab} + \frac{1}{4}w^b h_{ab} + \frac{1}{4}w_1^c h_{ab} = \frac{1}{4}w^a h_{ab} + \frac{1}{4}w^b h_{ab} + \frac{1}{2}w_1^c h_{ab},\\
\int_e f_2 \mathrm{d}s =& \int_a^b \Big[\frac{1}{h_{ab}}(b-s)w^a + \frac{1}{h_{ab}}(s-a)w^b + \frac{4}{h_{ab}^2}(s-a)(b-s)\Big(w_2^c - \frac{w^a+w^b}{2}\Big)\Big]\mathrm{d}s\\
=& \frac{2}{3}w_2^c h_{ab} + \frac{1}{6}w^a h_{ab} + \frac{1}{6}w^b h_{ab}.
\end{aligned}$$

In view of (3.5), the relation (3.1) follows.

For any $\zeta \in H^1(\widetilde{K})$, denote

$$c_1 := \frac{1}{|\widetilde{K}|}\int_{\widetilde{K}} \zeta \mathrm{d}\Omega \quad \text{and} \quad c_2 := \frac{1}{|e|}\int_e f_1 \mathrm{d}s,$$

also

$$c_2 = \frac{1}{|e|}\int_e f_2 \mathrm{d}s,$$

by (3.1). Then from trace inequality and Poincar*é* inequality, it follows

$$\begin{aligned}
&|\zeta - c_1|_{0,e} \lesssim h^{-\frac{1}{2}}\Big(|\zeta - c_1|_{0,\widetilde{K}}^2 + h|\zeta|_{1,\widetilde{K}}|\zeta - c_1|_{0,\widetilde{K}}\Big)^{\frac{1}{2}} \lesssim h^{\frac{1}{2}}|\zeta|_{1,\widetilde{K}},\\
&|f_1 - c_2|_{0,e} \lesssim h^{-\frac{1}{2}}\Big(|w - c_2|_{0,K_1}^2 + h|w|_{1,K_1}|w - c_2|_{0,K_1}\Big)^{\frac{1}{2}} \lesssim h^{\frac{1}{2}}|w|_{1,K_1},\\
&|f_2 - c_2|_{0,e} \lesssim h^{-\frac{1}{2}}\Big(|w - c_2|_{0,K_2}^2 + h|w|_{1,K_2}|w - c_2|_{0,K_2}\Big)^{\frac{1}{2}} \lesssim h^{\frac{1}{2}}|w|_{1,K_2}.
\end{aligned}$$

These three inequalities, together with (3.1), imply

$$\begin{aligned}
\Big|\int_e \zeta[w]\mathrm{d}s\Big| =& \Big|\int_e (\zeta - c_1)[w - c_2]\mathrm{d}s\Big|\\
&\le |\zeta - c_1|_{0,e}\big(|f_1 - c_2|_{0,e} + |f_2 - c_2|_{0,e}\big)\\
&\lesssim h|\zeta|_{1,\widetilde{K}}\big(|w|_{1,K_1} + |w|_{1,K_2}\big).
\end{aligned}$$

Taking

$$\zeta = \nabla u \cdot \mathbf{n},$$

in the above inequality and summing over all $e \in \mathcal{E}_h^*$, we obtain

$$\Big| \sum_{e\in\mathcal{E}_h^*} \int_e \nabla u \cdot \mathbf{n}[w] \mathrm{d}s \Big| \lesssim \sum_{\widetilde{K}\in\mathcal{T}_h^*} h|u|_{2,\widetilde{K}} \big(|w|_{1,K_1} + |w|_{1,K_2}\big) \leq h|u|_{2,\mathcal{T}_h^*} \|w\|_h,$$

which yields (3.4). □

Remark 3.3. Notice that the estimate of consistency error for the modified transition element is of $\mathcal{O}(h)$, while it is of $\mathcal{O}(h^{1/2})$ for the original transition element (cf. (2.12)).

With the modified shape functions (3.3), we still use

$$V_h := \Big\{ v : v|_{\Gamma_D} = 0, v \text{ is continuous at all the vertices other than hanging nodes of } \mathcal{T}_h,$$
$$\int_e v \mathrm{d}s \text{ is continuous over any transition edge } e,$$
$$v|_K = \left\{ \begin{array}{ll} v_{tr}, & \text{if } K \text{ is a 5-node transition element for all } K \in \mathcal{T}_h, \\ v_{bi}, & \text{if } K \text{ is a 4-node quadrilateral element for all } K \in \mathcal{T}_h, \end{array} \right\},$$

to denote the modified finite element space. Then, from Lemma 2.1, Eqs. (2.9), (3.4) and the standard interpolation theory, we have the following result.

Proposition 3.1. *Let $u \in V \bigcap H^2(\Omega)$ and $u_h \in V_h$ be respectively the solutions of the weak problem* (1.2) *and of the discretized problem* (2.7)*. Then it holds*

$$\|u - u_h\|_h \lesssim h|u|_{2,\Omega}.$$

4 Numerical tests

To verify performance of the modified nonconforming transition element, we consider the Poisson problem (1.1) over an L-shaped domain as shown in Fig. 6 (cf. [12]), where

$$\Omega = [-1,1]^2 \backslash [-1,0]^2, \qquad u = r^{\frac{2}{3}} \sin\Big(\frac{2\theta+\pi}{3}\Big),$$
$$\Gamma_D = \partial\Omega, \qquad f = 0.$$

For comparison we also compute the results of the conforming transition element [13] and the nonconforming transition element [8].

Test 1: Performance of the transition elements at given meshes.

We list the results of $\|u - u_h\|_h$ in Table 1 for different meshes shown in Fig. 6.

Test 2: Performance of the transition elements in h-refinement.

The initial mesh $\mathcal{T}_0$ is shown in Fig. 7. The h-refinement algorithm is as follows [3, 4]:

Loop for $l = 0, 1, 2, \cdots$, until termination on level L do:

1. Solve discrete problem (2.7) on $\mathcal{T}_l$;
2. $\forall K \in \mathcal{T}_l$, compute

$$\eta_K^2 := h_K^2 \|f + \mathrm{div}\nabla u_h\|_{L^2(K)}^2 + \frac{1}{2}\sum_{E\in\mathcal{E}(K)} h_E\Big(\|[\nabla u_h \cdot \mathbf{n}]\|_{L^2(E)}^2 + \|[\nabla u_h \cdot \mathbf{t}]\|_{L^2(E)}^2\Big),$$

where $\mathcal{E}(K)$ is the set of edges of K excluding $\partial\Omega$. Notice that

$$[\nabla u_h \cdot \mathbf{t}]\big|_E = 0,$$

if E is not a transition edge. Denote

$$\eta_N := \Big(\sum_{K\in\mathcal{T}_l} \eta_K^2\Big)^{\frac{1}{2}};$$

3. If

$$\eta_K > \frac{1}{2}\max_{T\in\mathcal{T}_l}\{\eta_T\},$$

mark K for bisection, output $\mathcal{T}_{l+1}$.

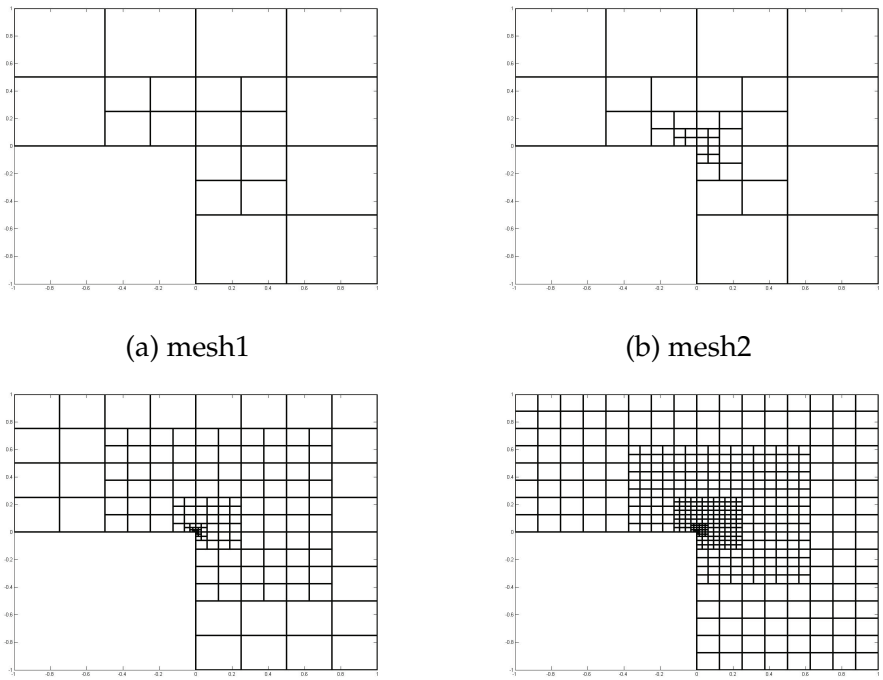

(a) mesh1 (b) mesh2

(c) mesh3 (d) mesh4

Figure 6: Meshes 1–4.

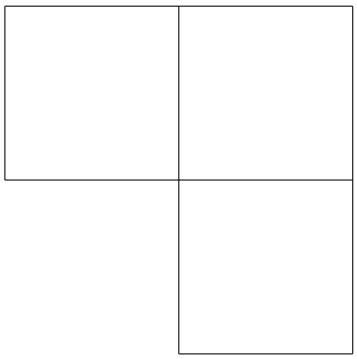

Figure 7: Initial mesh.

Table 1: The results of $\|u-u_h\|_h$ at different meshes.

	mesh1	mesh2	mesh3	mesh4
conforming transition element [13]	0.1046	0.0620	0.0288	0.0165
nonconforming transition element [8]	0.1156	0.0872	0.0516	0.0337
modified nonconforming transition element	0.1040	0.0604	0.0282	0.0162

Remark 4.1. In the mesh refinement, we also mark the element which has more than one mid-side node.

We show the relation between the number of d.o.f and the posteriori error η_N in Fig. 8.

As we can see from Table 1 and Fig. 8, the modified nonconforming transition element behaves better than its original version and the modified version is of the same accuracy as the conforming transition element by Gupta [13]. But, as pointed out

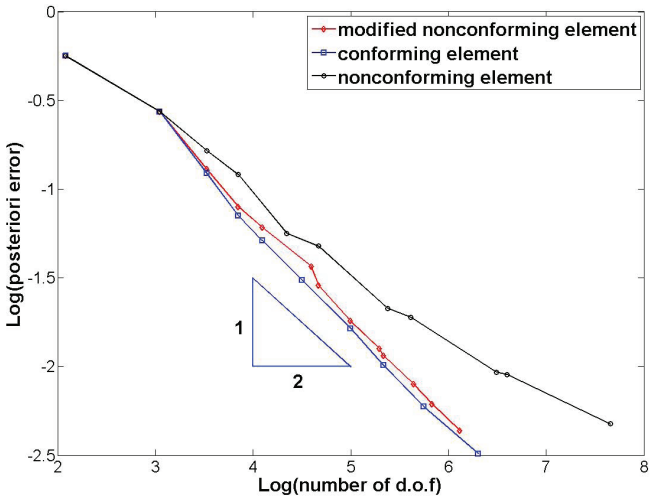

Figure 8: Relation of number of d.o.f and posteriori error.

in [13], for the conforming transition element, one has to use a modified quadrature formula to numerically integrate the gradient term of the stiffness matrix, since the interpolation functions for the conforming transition element are piecewise isoparametric bilinear over a transition element; while the modified nonconforming transition element, as well as its original version, has no such inconvenience.

Acknowledgments

This work was supported by Natural Science Foundation of China (10771150), the National Basic Research Program of China (2005CB321701) and the Program for New Century Excellent Talents in University (NCET-07-0584).

References

[1] ABEL J. F. AND SHEPHARD M. S., *An algorithm for multipoint constraints in the finite elemnt analysis*, Int. J. Numer. Meth. Eng., 14 (1979), pp. 464–467.
[2] BRENNER S. C. AND SCOTT L. R., The Mathematical Theory of Finite Element Methods, Springer-Verlag, New York, 1996.
[3] CARSTENSEN C. AND HU J., *A unifying theory of a posteriori error control for nonconforming finite element methods*, Numer. Math., 107 (2007), pp. 473–502.
[4] CARSTENSEN C., HU J. AND ORLANDO A., *Framework for the a posteriori error analysis of nonconforming finite elements*, SIAM. J. Numer. Anal., 45 (2007), pp. 68–82.
[5] CARSTENSEN C. AND HU J., *Hanging nodes in the unifying theory of a posteriori finite element error control*, J. Comput. Math., 27 (2009), pp. 215–236.
[6] CHOI C. K. AND LEE E. J., *Nonconforming variable-node axisymmetric solid element*, ASCE, 130 (2004), pp. 578–588.
[7] CHOI C. K. AND LEE N. H., *Three dimensional transition solid elements for adaptive mesh gradation*, Struct. Eng. Mech., 1 (1993), pp. 61–74.
[8] CHOI C. H. AND PARK Y. M., *Conforming and nonconforming transition plate bending elements for an adaptive h-refinement*, Thin. Wall. Struct., 28 (1997), pp. 1–20.
[9] CHOI C. K. AND PARK Y. M., *Nonconforming transition plate bending elements with variable mid-side nodes*, Comput. Struct., 32 (1989), pp. 295–304.
[10] CIARLET P. G., The Finite Element Method for Elliptic Problems, Amsterdam: North-Holland, 1978.
[11] DUAN M., MIYAMOTO Y., IWASAKI S. AND DETO H., *5-node hybrid/mixed finite element for Reissner-Mindlin plate*, Finite. Elem. Anal. Des., 33 (1999), pp. 167–185.
[12] ELMAN H. C., SILVESTER D. J. AND WATHEN A. J., Finite Elements and Fast Iterative Solvers: with Applications in Incompressible Fluid Dynamics, Oxford University Press, 2005.
[13] GUPTA A. K., *A finite element for transition from a fine to a coarse grid*, Int. J. Numer. Meth. Eng., 12 (1978), pp. 35–45.
[14] HASAN S. AND HASAN G., *A refined 5-node plate bending element based on Reissner-Mindlin theory*, Commun. Numer. Meth. Engng., 23 (2007), pp. 385–403.
[15] LEVIT I., NOUR'OMID B., STANLEY G. AND SWENSON G., *An adaptive mesh refinement strategy for analysis of shell structures*, Computational Structuratl Mechanics and Multi-

disciplinary Optimization, presented at The Winter Annual Meeting of the ASME, San Fransisco, CA, pp. 19–26, 1989.

[16] LO S. H., WAN K. H. AND SZE K. Y., *Adaptive refinement analysis using hybrid-stress transition elements*, Comput. Struct., 84 (2006), pp. 2212–2230.

[17] MCDILL J. M., GOLDAK J. A., ODDY A. S. AND BIBBY M. J., *Isoparametric quadrilaterals and hexahedrons for mesh-grading algorithms*, Commun. Appl. Numer. Method., 3 (1987), pp. 155–163.

[18] MORTON D. J., TYLER J. M. AND DORROH J. R., *New 3D finite element for adaptive h-refinement in 1-irregular meshes*, Int. J. Numer. Meth. Eng., 38 (1995), pp. 3989–4008.

[19] PETERS J. F. AND HEYMSFIELD E., *FEM formulation of four and five noded elements using a linearly varying stress assumption*, Int. J. Solid. Struct., 41 (2004), pp. 1991–2009.

[20] SOMERVAILLE I. J., *A technique for mesh grading applied to conforming plate bending finite elements*, Int. J. Numer. Meth. Eng., 6 (1972), pp. 310–312.

[21] WAN K. H., Transition Finite Elements for Mesh Refinement in Plane and Plate Bending Analysis, M.Phil.Thesis, Mechanical Engineering, The University of Hong Kong, 2004.

[22] WU D., SZE K. Y. AND LO S. H., *Two- and three-dimensional transition element families for adaptive refinement analysis of elasticity problems*, Int. J. Numer. Meth. Eng., 78 (2009), pp. 587–630.